Conformational and thermodynamical study of some helical perylenequinones

Leonardo Scaglioni,[a] Stefania Mazzini,[a] Rosanna Mondelli,*[a] Lucio Merlini,[a] Enzio Ragg[a] and Gianluca Nasini[b]

[a] *Dipartimento di Scienze Molecolari Agroalimentari, Sezione di Chimica, Università degli Studi di Milano, Via Celoria 2, 2013 Milano, Italy*
[b] *Centro del C.N.R. per le Sostanze Organiche Naturali, Dipartimento di Chimica, Politecnico di Milano, Piazza L. da Vinci 32, 20133 Milano, Italy*

Received (in Cambridge, UK) 3rd August 2001, Accepted 8th October 2001
First published as an Advance Article on the web 15th November 2001

Interest in polycyclic quinones derives not only from their photodynamic activity, but also from their possible application as antitumour and antiviral agents, in some cases as inhibitors of protein kinase C. A number of perylenequinones of natural origin are known, but the stereochemistry (they have a helical shape) and the interconversion process involving isomers with apparent opposed helicity, have not been sufficiently investigated. The conformational preference of the side-chains in the "1,12-bay" region, critical to generate the helical structure, was determined for perylenequinones **1**–**5** by the combined use of NOE data, of the two-bond and three-bond C,H and H,H coupling constants involving nuclei C-1, C-2, C-12b, C-15, 13-H and 14-H. As cercosporins **1**, **2** and phleichromes **3**, **4** possess a C_2 axis of symmetry, which reduces the number of available NMR parameters, an asymmetric derivative **5** (monoacetate of **1**) was prepared. Quantitative NOE experiments on **5** gave information on the relative distance of the two chains and on the twist angle C(1)–C(2)–C(12a)–C(12) of the helix. The noranhydro compounds **6** and **7** were obtained by treatment with sulfuric acid of cercosporins **1**, **2** and phleichromes **3**, **4**, respectively. The structure and the conformational preference of **6** and **7** were deduced by NMR at low temperature, by CD spectra and molecular modelling. The thermal inversion of the helix was studied by traditional kinetic experiments for **1**–**4** (the process is slow even at high temperature), by NOESY-exchange and dynamic NMR experiments for **6** and **7**. The activation parameters $\Delta H^{\#}$, $\Delta G^{\#}$, and $\Delta S^{\#}$ were thus obtained. The helix inversion process results tightly connected with the conformational change of the side-chains of the atropisomers, but not with the tautomeric state of the perylenequinone system.

Introduction

Interest in polycyclic quinones stems not only from their peculiar structural features, but also from their photodynamic activity.[1–4] One of them, cercosporin **1**, is an efficient singlet oxygen producer,[5] whereas other 4,9-dihydroxyperylene-3,10-quinones belonging to the cladochrome group[6] have been shown[7] to be potent inhibitors of protein kinase C, thus hinting at possible antitumour and antiviral activity.[8] More recently, hydroxyphenanthroperylenequinones, such as hypericin and stentorin, have been investigated,[9] owing to their biological properties with possible applications as antiviral drugs. We have studied[6,10] a number of perylenequinones of natural origin and several derivatives, with regard to structure elucidation, tautomerism and synthetic modifications. The perylenequinone moiety in these compounds is not planar, but assumes a helical shape, which generates axial chirality. Thus, the stereochemistry and the interconversion process involving isomers with apparent opposite helicity still present some fascinating aspects. In particular, the conformation of the side-chains, so critical to induce the steric strain that forces the polycyclic ring into the helical shape, has not been sufficiently investigated.

Cercosporins and phleichromes **1**–**4**, produced *via* a common biosynthetic pathway, show similar structural elements: two bulky methoxy groups or a strained seven-membered ring in positions 6 and 7, two C_3 side-chains in positions 1 and 12 and a non-planar helical shape. The helicity generates axial chirality, which when associated with the presence of asymmetric carbon atoms in the side-chains gives rise to diastereoisomerism.[4] The thermal isomerisation of cercosporin **1** into the diastereoisomer isocercosporin **2** was correctly explained[11] by the inversion of the ring helix, on the basis of CD and ORD evidence. This was confirmed by X-ray analyses,[10a,12] that also defined the *RR*

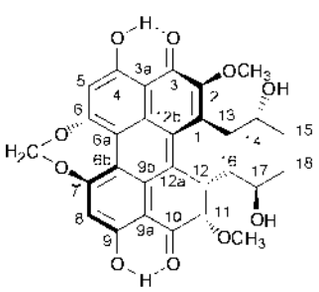

1 (Helix *M*, 14*R*, 17*R*]

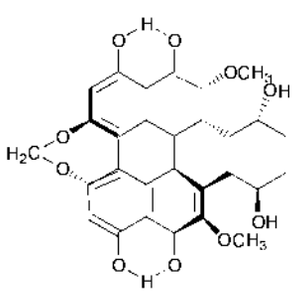

2 (Helix *P*, 14*R*, 17*R*)

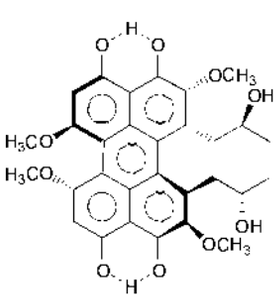

3 (Helix *P*, 14*S*, 17*S*]

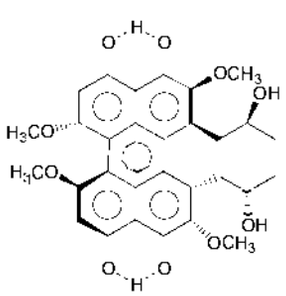

4 (Helix *M*, 14*S*, 17*S*]

 DOI: 10.1039/b107071c

Table 1 Selected H,H and C,H coupling values (Hz) for compounds **1**–**5**[a]

J	**1**	**2**	**3**	**4**	**5**[b]	**5**[c]	
H13a, H13b	13.0	13.0	12.5	13.1	12.8	H16a, H16b	13.6
H13a, H14	6.0	3.5	6.0	3.5	5.9	H16a, H17	5.7
H13b, H14	7.0	8.5	7.5	8.7	7.2	H16b, H17	6.8
C1, H13a	5.5	5.4	5.6	5.5	5.5	C12, H16a	5.6
C1, H13b	5.5	5.4	5.6	5.5	5.5	C12, H16b	5.6
C1, H14	1.8	2.4	1.8	2.2	1.8	C12, H17	2.9
C2, H13a	3.2	3.4	3.2	3.3	3.4	C11, H16a	3.4
C2, H13b	6.3	5.8	6.0	6.0	5.9	C11, H16b	5.8
C12b, H13a	6.2	5.8	5.8	5.6	6.2	C12a, H16a	6.2
C12b, H13b	3.1	3.1	3.2	3.3	3.0	C12a, H16b	2.8
C15, H13a	5.4	2.5[d]	5.6	2.5	5.4	C18, H16a	4.1
C15, H13b	3.2	3.3[d]	3.2	3.2	3.2	C18, H16b	4.1
C15, H14	1.3	1.3	1.2	1.2	≤1.0	C18, H17	1.7

[a] Measured in [$^2H_6$]acetone at 25 °C from Me_4Si. Concentration 5–7 × 10^{-2} mol dm^{-3}. Estimated accuracy ±0.1 Hz unless specified. Ha and Hb refer to lowfield and upfield proton respectively. Ha is *pro-R* for **1**, **4** and **5**; whereas it is *pro-S* for **2** and **3**. [b] Not acetylated chain. [c] Acetylated chain. [d] Measured from the decoupled spectrum upon irradiation of 14-H (accuracy ±0.2 Hz).

configuration at C-14 and C-17 of **1** and the sign of the axial chirality as *M*.[10a] Consequently, isocercosporin **2** has *P* axial chirality and *R* configuration of the side-chain carbons.[4] The same behaviour is presented by phleichrome **3**, which equilibrates with isophleichrome **4**.[10b] Here, however, the natural isomer has *P* axial chirality and *S* configuration of the side-chain carbons, as shown by the CD curve and *via* Horeau's method respectively.[10b] That the side-chains of the two diastereoisomers **1** and **2** possess different conformations in solution, was initially suggested by the chemical shifts of the methyl groups on the side-chains and by the values of the coupling constants between 13-H and 14-H.[11] Unfortunately, these structures possess a C_2 axis of symmetry, lying in the main plane of the molecule, which makes the corresponding atoms in the two halves chemical shift equivalent. † Consequently the number of the NMR parameters available for the conformational analysis was greatly reduced; in particular the interactions between the two chains were not detectable. Thus, we synthesised an asymmetric compound **5**, in order to measure the cross-relaxation rates involving protons of the two chains, which can be converted into interproton distances. This paper reports the results of a conformational and thermodynamical study performed on cercosporin **1**, isocercosporin **2**, phleichrome **3**, isophleichrome **4**, cercosporin monoacetate **5**, noranhydrocercosporin **6** and noranhydrophleichrome **7**.

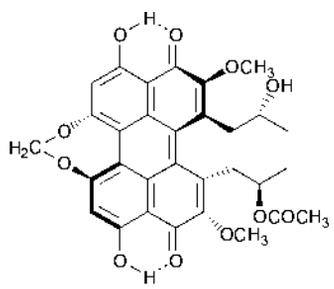

5 (Helix *M*, 14*R*, 17*R*)

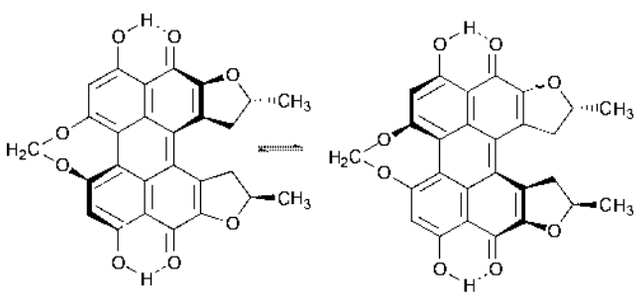

I (Helix *M*, 14*R*, 17*R*) II (Helix *P*, 14*R*, 17*R*]

6

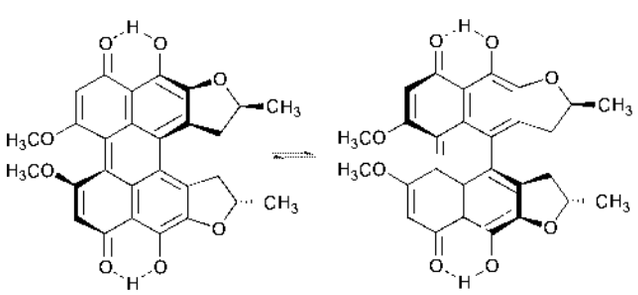

I (Helix *M*, 14*S*, 17*S*) II (Helix *P*, 14*S*, 17*S*]

7

Results and discussion

Conformational analysis of compounds 1–5

First we studied the rotation around bonds C(1)–C(13) and C(13)–C(14) by using the H,H and ^{13}C,H coupling constants values reported in Table 1. The assignment of carbon and proton resonances for **1**–**4** has already been reported,[10d] but not the stereospecific assignment of the geminal protons at C-13, which was thus performed by NOE experiments (Table 2). Selected chemical shift values for **1**–**5** are also reported in Table 2. The irradiation of the 2-OMe protons gave 0.5–1.0% enhancements of the lowfield 13-Ha resonance for compounds **1**–**5**, while the signal of the geminal partner, 13-Hb, was almost unaffected. The inverse experiments, *i.e.* the irradiation of the protons at C-13, confirmed these results. Thus, it follows that the lowfield 13-Ha is oriented toward the methoxy group at C-2 and consequently is *pro-R* in **1**, **4** and **5**, whereas it is *pro-S* in **2** and **3**.

The preferred conformation around bond C(1)–C(13) can be deduced from the values of ^2J(C1,H13), ^3J(C2,H13) and ^3J(C12b,H13) (Table 1). The geminal coupling between aromatic carbons (αC) and benzylic protons (αH) is known[13] to depend on the orientation of the αC–αH bond, with respect to the π orbital of the aromatic ring. The same value of ^2J found for the two protons at C-13 indicates that they are symmetrically oriented with respect to the aromatic system (Fig. 1). Such

† Therefore, in the following discussion, mention of a particular H or C atom of the "upper" part of the molecule for compounds **1**–**4** will include the corresponding atom of the "lower" part.

Table 2 Stereospecific assignment (δ) and NOE enhancements (%) of 13-H and 16-H resonances for compounds **1**–**5**[a]

Chemical shift[b]	**1**	**2**	**3**	**4**	**5**	**5**
13-H *proR*	3.65	2.97	2.91	3.49	3.68	3.71[d]
13-H *proS*	2.93	3.51	3.65	2.95	2.89	3.13
14-H	3.42	3.61	3.44	3.64	3.45	4.65
15-H_3	0.47	0.99	0.31	0.98	0.63	0.52
NOE %[c]	**1**	**2**	**3**	**4**	**5**	**5**
13-H *proR*	0.84	0.15	0.30	0.56	0.98	0.76[d]
13-H *proS*	0.30	0.54	0.91	0.20	0.23	0.25
14-H	0.91	1.05	1.12	0.88	1.8	1.8

[a] ^{2}[H_6]Acetone. Concentration as in Table 1. [b] Measured at 25 °C from Me_4Si. Accuracy within ±0.01 ppm. [c] Steady state NOE experiments on irradiation of 2-OMe resonance. These experiments were preferred with respect to NOESY, because of the low NOE values, always expected when methyl groups are involved. [d] The values of this column refer to the protons of the acetylated side chain, *i.e.* 16-H_2, 17-H and 18-H_3.

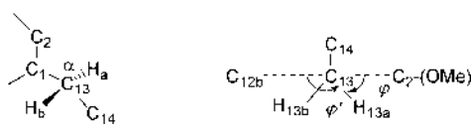

Fig. 1 Projection of C(14)–CH_2(13)–C(1)–C(2)–C(12b) along the vector ***C(13) ⋯ C(1)***. For all compounds 13-Ha, cisoid to 2-OMe, resonates at low field. 13-Ha is *pro-R* for **1**, **3** and **5**, *pro-S* for **2** and **3**.

a conformation requires dihedral angles C(2)–C(1)–C(13)–H(13a) = C(12b)–C(1)–C(13)–H(13b) ~ 30°, because the alternative conformation with angles of 150° is too much sterically hindered. The measured coupling constants of 5.4–5.6 Hz are in agreement with the value (6.48 Hz) calculated for toluene with an angle of 30°.[13] The vicinal coupling between benzylic protons and aromatic carbon atoms depends on the relative orientation of the coupled nuclei, following an angular dependence which differs from the Karplus equation.[13,14] It has been found[13,14] that the interactions are lower for cisoid relationships than for transoid ones. The values of J(C2,H13a) = J(C12b,H13b) = 3.1–3.4 Hz and J(C2,H13b) = J(C12b,H13a) = 5.8–6.0 Hz suggest that for **1**–**5** the atoms in each pair, 13-Ha/C-2 and 13-Hb/C-12b, are cisoid, while those in the other pair are transoid, *i.e.* the φ angle is smaller than φ'. In addition, the similar values found for each pair of couplings and the values of the corresponding ^2J (5.4–5.6 Hz) and ^3J (3.5 and 5.0 Hz) measured in elsinochromes,[10c] where 13-H is equatorial on a six-membered ring closed on C-1 and C-11 with φ = 30° and φ' = 140°, confirm the geometry reported in Fig. 1.

The preferred conformation around bond C(13)–C(14) was then deduced from the vicinal H,H and C,H coupling constants, namely J(H13*R*,H14), J(H13*S*,H14), J(C1,H14), J(C15,H13*R*), J(C15,H13*S*). We used the Karplus type equation proposed and successfully applied by Altona,[15] Schaefer,[14] Barfield[16] and co-workers. Following their models and considering also the values for norbornane[17] and cyclohexanol,[18] we used in the fragments ^{13}C(1)–CH_2(13)–CH(14)–OH and CH_2(13)–CH(14)–^{13}C(15) the following limiting J values. For J(H13,H14), J^{180} = 11.4 Hz, J^{+60} = 3.2 Hz (when the OH group is *gauche* to H-13, positive *gauche* effect[15]), J^{-60} = 2.0 Hz (in the absence of *gauche* effect). For J(C1,H14) and J(C15,H13) we used J^{180} = 8.0 Hz, J^{60} = 2.1 Hz (with *gauche* effect), J^{60} = 1.1 Hz (without *gauche* effect).

The populations relative to the three main conformers *trans*, *gauche*$^-$ and *gauche*$^+$ (Fig. 2 and Table 3) were then obtained by solving the appropriate linear equation with the least-squares method (see Experimental). These results show that the side-chains have a certain mobility, all the three main conformations being populated. However, some of these conformers are selectively preferred. Cercosporin **1** and phleichrome **3** prefer

Table 3 Relative populations of the three main conformers around bond C(1)–C(13) for compounds **1**–**5**

Me–C(1)	*trans*	*gauche*$^+$	*gauche*$^-$
1	0.35	0.53	0.15
2	0.67	0.16	0.18
3	0.34	0.13	0.58
4	0.69	0.12	0.17
5	0.33	0.54	0.15
5[a]	0.32	0.43	0.31

[a] These values refer to the protons of the acetylated side chain.

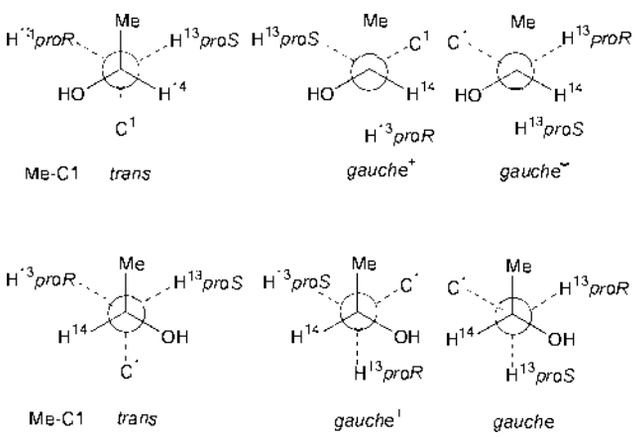

Fig. 2 Newman projections along C(14)–C(13) of the main conformers for compounds with 14*R* configuration, **1**, **2** and **5** (on the top) and for compounds with 14*S* configuration, **3** and **4** (on the bottom). Only one chain is represented, as the chiral centre on the other chain, C-17, has the same configuration. Names are referred to the Me–C_1 relationship.

the *gauche*$^+$ and the *gauche*$^-$ conformation respectively, even though the *trans* one is also present. In contrast, isocercosporin **2** and isophleichrome **4** definitely prefer the *trans* conformation. Cercosporin monoacetate **5** shows for the non-acetylated chain the same situation as cercosporin **1**, while for the acetylated chain the three conformations appear equally populated. The *gauche*$^+$ conformer for **1**, as well as the *gauche*$^-$ for **3**, displays the methyl groups curled back toward the perylenequinone system, whereas in the *trans* conformer, the methyls are oriented to the opposite side. This explains the chemical shift values of the methyl protons, which are shielded in **1** and **3**, but not in **2** and **4**, by the ring current effect of the aromatic system. This is clearly visible in Fig. 3a and 3b, which represent the conformation *gauche*$^-$ of phleichrome **3**, and the conformation *trans* of isophleichrome **4**, respectively. In the case of cercosporin monoacetate **5**, the 15-Me protons show the same shift as in **1**, while 18-Me is slightly less shielded. This is in agreement with an increased population of the *gauche*$^-$ form, with respect to **1**, as reported in Table 3. The shift of the acetyl group (1.54 ppm) also reflects this situation, and shows a slight up-field effect by the aromatic system.

The NOE experiments confirm these results. In steady-state NOE measurements strong interactions of 15-Me protons with 13-H *proS*, but not with 13-H *proR*, were found in compounds **1**, **3** and **5**. In contrast, in the atropisomers **2** and **4**, the interactions of the methyl protons with 13-H *proS* and 13-H *proR* are approximately the same. In order to take into account the third-spin effect, usually observed in this kind of spin system, we performed 1D-transient NOE and 2D-NOESY experiments at different mixing times, which allowed the measurement of the cross-relaxation rates involving the above said protons. The NOEs observed between 13-H *proR* and 13-H *proS* and between 14-H and 15-Me protons were used as a reference, thus transforming the measured cross-relaxation rates into "apparent distances" (see Experimental). In the presence of different

Table 4 Interproton distance values (Å) for cercosporin monoacetate **5**[a]

Distances	Exp.[b]		Calc.	
	[c]	[d]	[e]	[f]
13-H *proR* ··· 16-H *proR*	[g]	[g]	3.55	
13-H *proS* ··· 16-H *proR*	2.44	[g]	2.80	
13-H *proR* ··· 16-H *proS*	2.63	[g]	2.78	
13-H *proS* ··· 16-H *proS*	2.41	2.31	2.51	
13-H *proR* ··· 14-H	2.80	2.56	2.97	2.49
13-H *proS* ··· 14-H	2.63	2.57	2.57	2.55
16-H *proS* ··· 17-H	2.39	2.31	2.51	2.53
16-H *proR* ··· 17-H	2.58	2.44	2.78	2.53
13-H *proR* ··· 15-Me	3.10	3.40	3.58	3.21
13-H *proS* ··· 15-Me	2.82	2.83	2.60	3.00
16-H *proR* ··· 18-Me	3.26	3.03	3.20	3.11
16-H *proS* ··· 18-Me	2.92	2.95	2.92	3.05
14-H ··· 2-OMe	3.20	3.54	3.60	
17-H ··· 11-OMe	3.51	3.87	3.95	
13-H *proR* ··· 2-OMe	3.05	2.96	3.27	
13-H *proS* ··· 2-OMe	[h]	[h]	4.54	
16-H *proR* ··· 11-OMe	3.15	3.05	3.37	
16-H *proS* ··· 11-OMe	[h]	[h]	4.86	
13-H *proS* ··· 11-OMe	[h]	[h]	4.66	
16-H *proR* ··· 2-OMe	[h]	[h]	4.39	

[a] The distance (1.75 Å) between the geminal protons at C-13 and C-16 was taken as reference, except for the interactions involving methyl groups, in this case the distance (2.5 Å) between 14-H and 15-Me was used. [b] Obtained from 2D-NOESY experiments and by the use of Felix software. [c] In $CDCl_3$. [d] In [$^2H_6$]acetone. [e] Calculated by MM/MD procedure. [f] Obtained from the averaged NOE values, calculated over the three main conformers of Fig. 2, with the relative populations derived from the coupling constants in acetone solution. [g] Not detected because the signals are too close or overlapping. [h] Zero NOE.

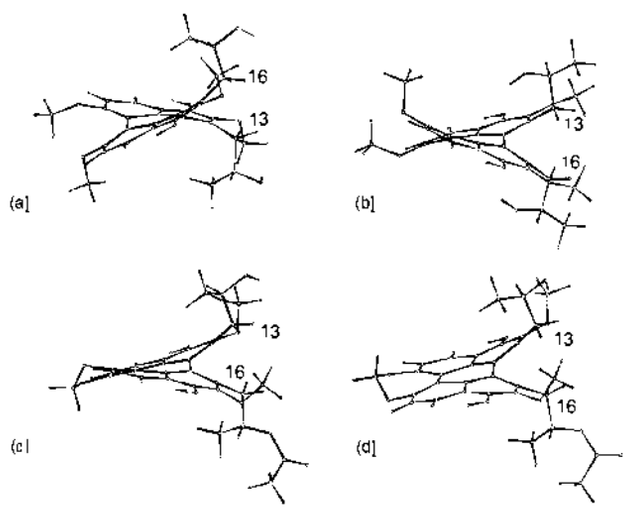

Fig. 3 (a) *gauche*$^-$ conformation of phleicrome **3**, (b) *trans* conformation of isophleichrome **4**, (c) one of the "propeller" conformations of cercosporin monoacetate **5**, obtained from NOE experiments and molecular modelling, (d) "double butterfly" conformation of **5**, obtained from molecular modelling.

conformations, the measured inter-atomic distances do not correspond to protons situated at "fixed" geometries and should be considered as "apparent", as they originate by weighted averages over all populated conformers. We thus analysed the NOE data, by taking into account ideal dihedral angles corresponding to the classical *gauche* and *trans* conformations.

The NOE results are in agreement with those obtained from coupling constant values. As an example, we report in Table 4 the data of cercosporin monoacetate **5**. The NOE experiments performed on the asymmetric derivative **5** also gave information on the relative distances of the two chains, allowing detection of the interactions between protons of the two different chains. The distance values thus obtained were used as restraints for

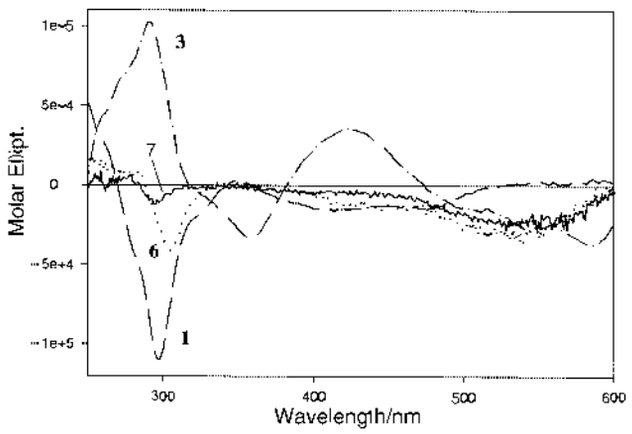

Fig. 4 CD spectra of (— —) cercosporin **1**, (— · —) phleichrome **3**, (.....) noranhydrocercosporin **6** (×2) and (——) noranhydrophleichrome **7** (×2).

molecular modelling. MD calculations led to a set of structures that, after minimisation, converge to the structure shown in Fig. 3c. Specifically, the molecule presents a helical shape with the twist angles C(1)–C(12b)–C(12a)–C(12) and C(6)–C(6a)–C(6b)–C(7) of −36° and −15°, respectively; one of the side-chains is bent upward, the other downward, with respect to the perylenequinone system. The NOE interactions between the side-chains and the 2-OMe and 11-OMe protons also allowed sketching of the preferred conformation of the two methoxy groups, as shown in the figure. In the solid phase, the X-ray analysis[12] of cercosporin **1** showed a similar helical structure with twist angles of −29.84° and −9.17°, respectively. This conformation was called "propeller" by Falk and co-workers[19] (Fig. 3c), who also calculated that this conformation is more stable than the other one called "double butterfly" (Fig. 3d) and having twist angles of −30° and +20°, respectively. Our calculations confirm this finding, the "propeller" structure being found to be more stable by 7.2 kJ mol^{-1}.

Conformational analysis and stereochemistry of noranhydro derivatives 6 and 7

Noranhydrocercosporin **6**[10a,11,20] was prepared by treatment with concentrated sulfuric acid of cercosporin **1** or isocercosporin **2**; likewise, noranhydrophleichrome **7** was obtained from phleichrome **3** or isophleichrome **4**. The structure of **6** and **7** was deduced on the basis of the NMR and CD spectra. The NMR spectra indicate that **6** and **7** possess a C_2 axis of symmetry lying in the main plane of the molecules and show the presence of the chelated phenolic hydroxy groups, of the methyl groups and of the three protons on each side-chain, while two OMe groups are missing.

The low intensity of the CD spectrum of **6** in comparison with that of **1** and **2** (Fig. 4) had first suggested[10a] that the perylenequinone system is planar. Actually the folding of the side-chains to form the dihydrofuran rings significantly lowers the inversion barrier, so that, at room temperature and down to −40 °C, the NMR spectrum of **6** still shows sharp resonances; the two atropisomers are in a fast equilibrium regime and therefore the opposite Cotton effects due to the atropisomers are averaged in the CD spectrum. Lowering the temperature, the NMR signals become broader and broader, and only at −93 °C are two separate and almost sharp resonances obtained for each proton species. The NMR spectrum of **7** shows separate but broad signals at room temperature, that become sharp at −5 °C. The two atropisomers display different populations, *i.e.* 79 : 21 for **6** and 62 : 38 for **7**.

The configurational identity of the stereogenic centres in the side-chains might be retained or lost, depending on the mechanism of the cyclisation. This is awkward to predict *a priori*, and

Table 5 Selected chemical shift (δ) and coupling constant (Hz) values for compounds **6** and **7**

	Chemical shift					*J*			
	6[a]		**7**[b]			**6**[a]		**7**[b]	
Atropisomers	I	II	I	II		I	II	I	II
13-H *proR*	2.92	3.57	3.31	4.15	H13 *proR*, H14	13.0	7.0	7.5	9.2
13-H *proS*	3.88	3.33	3.58	2.91	H13 *proS*, H14	8.0	9.0	12.0	4.0
14-H	5.32	5.09	4.84	5.32	C3, OH	—		4.5	4.0
					C4, OH	5.0[c]		2.0	2.4

[a] Measured at −80 °C in $CDCl_3$–$CFCl_3$ (30 : 70); relative population of atropisomers I, 79%, II, 21%; conc. 7×10^{-3} mol dm^{-3}. [b] Measured at −5 °C in $CDCl_3$; relative population of atropisomers I, 62%, II, 38%; conc. 4×10^{-2} mol dm^{-3}. [c] Measured at room temperature.

an experimental determination would be very difficult, except *via* an X-ray analysis. However, the existence of only two atropisomers in fast equilibrium and the low, but not zero, intensity of the CD spectrum at room temperature indicate that the configuration of both stereogenic centres must be retained or inverted. In both cases, the fast inversion of the helix gives rise to two atropisomers in fast equilibrium, and the CD spectrum, where the contribution of the axial chirality is overwhelming, is averaged to a low intensity due to the chirality of the centres of the chains. In the case of a mixture of the two compounds with *RR* and *SS* configuration, the inversion of the helix puts them in an enantiomeric relationship, so that again only two, and not four, atropisomers would appear in the NMR spectrum. On the contrary, had racemisation of the centres occurred, due to protonation of the hydroxy groups of the chains and cyclisation *via* a carbocation, three isomers, instead of two, would have been observed in the NMR spectrum. Moreover, HPLC of **6** and **7** on a chiral phase column showed only one peak, consistent with the hypothesis of retention or inversion of both the stereogenic centres. A complete inversion of the stereogenic centres in the side chains appears unlikely in the acidic cyclisation conditions, whereas retention of the configuration is consistent with protonation of the methoxy groups, intramolecular cyclisation to form an acetal and loss of MeOH. Such a mechanism of exchange of ethyl groups of polycyclic alkyl aryl ethers in alcoholic acid has been recently discussed.[21]

In the CD spectrum of **6** (Fig. 4) there is a clear Cotton effect around 300 nm, similar to that shown by cercosporin **1**. As the ratio of the two atropoisomers is 79 : 21, and the contribution of the axial chirality is overwhelming, it follows that the more abundant atropoisomer of **6** must have the *M(R)* configuration. The CD spectrum of **7** is also of cercosporin type, but the intensity is lower than for **6**, in agreement with the smaller difference in the populations of the atropisomers (62 : 38).

Calculations performed with the Insight II & Discover program on the two atropisomers of **6** show that the structure *M(R)*, *RR* is more stable (*ca.* 8.6 kJ mol^{-1}) than *P(S)*, *RR*. This is in agreement with the above suggested mechanism of cyclisation and allows the proposal of the configuration *M(R)*, *RR* for the more abundant (I) atropisomer of **6** and thus the configuration *P(S)*, *RR* for the less abundant one (II). An examination of the chemical shifts of the most significant protons for **6** and **7** (Table 5) shows that the less abundant atropisomer of **6** has similar values to those of the more abundant atropisomer of **7**, and the same relationship occurs for the other two atropisomers respectively. The correlation between the corresponding protons in the two atropisomers, and thus the assignments reported in the Table, were performed by NOE-exchange experiments. These data show that isomer I of **6** and isomer II of **7** must have the same configuration, or that they are in a pseudo enantiomeric relationship. Thus, the atropisomer II of **7** must be *M(R)*, *RR* or *P(S)*, *SS*. As the CD spectrum of **7** is of cercosporin type, *i.e.* with a predominant *M(R)* configuration, the less abundant atropisomer II of **7** is *P(S)*, *SS* and consequently the more abundant one (*I*) is *M(R)*, *SS*. The calculations confirm these results; in the case of **7**, the structure *M(R)*, *SS* is more stable by *ca.* 8.8 kJ mol^{-1} compared with the *P(S)*, *SS* one. This is in agreement with a retention of configuration of the stereogenic centres of the side-chains, as discussed above.

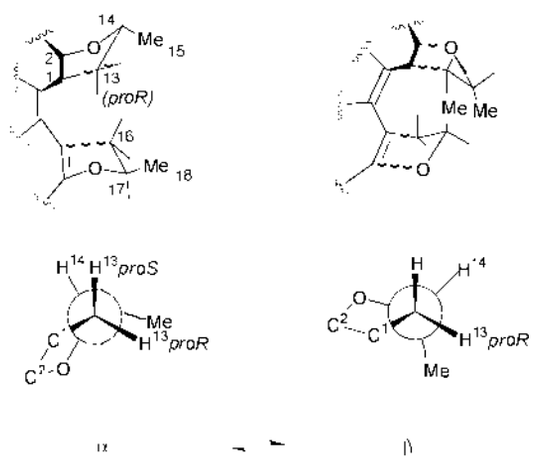

Fig. 5 Two envelope conformations of the five-membered rings for noranhydro derivatives **6** and **7**, in the case of a configuration *M(R), 14R, 17R*.

The H,H coupling constants measured at low temperature from the separate signals of each atropisomer of **6** and **7** (Table 5) gave further information. The more stable atropisomer of **6** shows a large coupling constant (13 Hz) between 14-H and one of the protons at C-13, which indicates a pseudo-diaxial relation with a dihedral angle Φ very close to 180°. The coupling constant with the other 13-H (8.0 Hz) indicates an angle Φ' less than 60°. The conformational mobility of five-membered rings is described by the so-called pseudorotational process,[22,23] but the lock of two carbon atoms on the perylenequinone system reduces the motion to an "out of plane" oscillation of only one atom (C-14). Thus, two envelope conformations α and β can be considered, *i.e.* those where C-14 is up or down with respect to the O–C(2)–C(1)–C(13) plane. The corresponding Newman projections, in the case of a configuration *M(R), 14R, 17R* are reported in Fig. 5. Calculations performed with a Karplus-type equation modified by Altona and co-workers[15] gave Φ‡ = 170–180° and Φ' = 30–35°, values supporting conformation α for the more abundant atropisomer of **6**. This conformation displays 15-Me and 18-Me in pseudo-equatorial positions.

The inversion of the five-membered ring leads to a less stable form, because the methyl groups become pseudo-axial. This explains the high preference for conformation α. The less stable

‡ Φ = H(14)–C(14)–C(13)–H(13*proR*); Φ' = H(14)–C(14)–C(13)–H(13*proS*) for **6**. In the case of **7**, Φ is the angle with 13-H *proS* and Φ' with 13-H *proR*. A better fitting was obtained when the electronegativity of the enol-ether oxygen atom is considered similar to that of a carbon atom.

Table 6 Rate constants (k) for the helix inversion process of perylenequinones [a]

1 [b]		**3** [b]		**6** [c]				**7** [c]			
T/°C	$k \times 10^5$/s^{-1}	T/°C	$k \times 10^5$/s^{-1}	T/°C	k/s^{-1}	T/°C	k/s^{-1}	T/°C	k/s^{-1}	T/°C	k/s^{-1}
83	3.6	148.7	25.8	−100	2.1	−84 [d]	45	−28 [d]	0.1	+11 [d]	24
102.7	21.6	155.4	45.0	−93	10	−79	89	−20	0.4	+14 [d]	38
109.3	41.6	160.5	61.6	−93 [d]	12	−79 [d]	90	−16 [d]	0.6	+20	51
119.1	86.2	165.8	74.5	−89 [d]	16	−75 [d]	165	−10	2.0	+21 [d]	80
123.4	122.6	170.8	108.7	−85	37	−65 [d]	700	−5 [d]	3.0	+30 [d]	200
128.1	208.0	183.9	256.6	−85 [d]	35	−57 [d]	1800	0	5.6	+40 [d]	540
135.3	330.6							+7 [d]	14	+45 [d]	800
								+10	16	+50 [d]	1150

[a] Estimated error within 5%. [b] Kinetic experiments performed by heating in DMSO and collecting samples at intervals for NMR measurements. [c] From NOE-exchange experiments, unless otherwise specified. Solvent, $CDCl_3$–$CFCl_3$ (30 : 70) for **6** and $CDCl_3$ for **7**. [d] From line-shape analysis.

Table 7 Activation parameters for the helix inversion process of perylenequinones [a]

	$\Delta G^{\#}_{298}$/kJ mol^{-1}	$\Delta H^{\#}$/kJ mol^{-1}	$\Delta S^{\#}$/J mol^{-1} K^{-1}
1	115.8	103.6 ± 0.2	−41.0 ± 0.5
3	123.1	98.6 ± 0.7	−82.4 ± 1.6
6	35.8	46.4 ± 0.2	35.3 ± 0.6
7	61.3	76.3 ± 0.2	50.2 ± 0.4

[a] The reported errors are standard deviations, obtained from the regression analysis. More realistic values might be three times the standard deviations, which also corresponds to statistical uncertainties calculated by considering ±1 °C fluctuations in the temperatures.

atropisomer shows coupling constant values of 7.0 and 9.0 Hz, which suggests that they are averaged values. If we assume relative populations of 70% and 30% for the α and β form respectively, we obtain calculated averaged coupling constants of 7.0 and 8.0 Hz, which are in good agreement with those measured for 2,3-dihydro-2-methylbenzofurans[24] and with our experimental values. The preferred conformation of the more abundant (I) atropisomer of **7** is represented by the β form, but with the methyls in a pseudo-equatorial orientation, as results from the coupling constant values (12.0 and 7.5 Hz) of 13-H_2 and 14-H protons. The less abundant isomer II shows J values of 4.0 and 9.2 Hz, which correspond to dihedral angles of *ca.* 120° and 10–20° (obtained by the Karplus equation) and indicate that the preferred conformation is represented by the α form, but with the methyls in a pseudo-axial orientation.

Helix inversion process

The thermal inversion of the helix in cercosporin and phleichrome is a slow process even at elevated temperatures. The barrier cannot be estimated by dynamic NMR experiments, because even heating at 150 °C a mixture of **1** and **2** or of **3** and **4** did not induce any coalescence of the signals of the isomers in the NMR spectrum. Therefore, we measured the rate constants of the interconversion of **1** and **3** at different temperatures by collecting samples at intervals for NMR measurements, which gave the relative concentration of the two atropisomers (see Experimental). The activation parameters were obtained by least-squares fits of $\ln(k/T)$ *vs.* $1/T$ data from the Eyring and the Gibbs–Helmholtz equations[25,27] (see Experimental). The values of the rate constants, of $\Delta H^{\#}$, $\Delta G^{\#}$ and $\Delta S^{\#}$ are reported in Tables 6 and 7. Different values of $\Delta H^{\#}$ and $\Delta S^{\#}$ had been obtained previously[10a] for cercosporin **1** through a different procedure, which was found to be less accurate. The high values of the negative entropy change can be attributed to the change of conformation of the side-chains in the interconversion process, and can explain the long half-time for the isomerisation, with an energy barrier not too different from that of other faster interconverting systems.[22] Compared to the atropisomers **1**–**2**, the couple **3**–**4** shows a higher barrier, which can be explained by the more crowded situation occurring in the "bay" region (positions 6 and 7), due to the presence of the two methoxy groups instead of the methylenedioxy group. The important role of the interactions of the side-chains and of their conformational changes towards enhancement of the energy barrier is shown by the fact that cyclisation of the side-chains in the noranhydro derivatives **6** and **7** reduces the barrier.

The helix inversion process for compounds **6** and **7** was studied by NOESY-exchange experiments[26] and by classical dynamic NMR Spectroscopy (DNMR) with line-shape analysis,[27] as the interconversion between the atropisomers is fast enough with respect to the NMR timescale. The first method is highly preferred, when possible, because the errors introduced are relatively small, providing that the separation of the exchanging signals allows measurement of good integrals. The interconversion rate constants (k) were directly determined by quantification of the signal intensities of diagonal and cross peaks of the NOESY spectra, performed at different mixing times. The k values result by fitting of the experimental data in the appropriate equations (see Experimental). The DNMR method requires an accurate choice of the reference half-widths, *i.e.* the half-width of the slow exchanging proton signals and a precise quantification of the parameters—other than the rate constants—that affect the line-width of the signals, especially at very low temperatures, for instance the viscosity of the solution and the inhomogeneity of the magnetic field.

The 2D-NOESY spectrum of noranhydrocercosporin **6** performed at −93 °C is reported in Fig. 6 as an example. The signals of the chelated phenolic OH protons in this compound are the most appropriate to be monitored, because of the larger chemical shift difference; the chemical exchange with water was checked and excluded at low temperatures down to −50 °C. The line-width of the OH resonances was also monitored on noranhydrophleichrome **7**: down to −20 °C it is the same as that of the 5-H signals. The NOESY experiments on **7** were performed at temperatures between −20 and +20 °C by using both the 5-H and OMe signals and the rate constant values obtained are in good agreement. The spectra for DNMR investigations, recorded at different temperatures, were then carefully simulated and iterated by line-shape analysis. Selected parts of the experimental and the simulated spectra are reported in Fig. 7. The rate constant values obtained with the two methods are in satisfactory agreement (Table 6).

The k values were then used for the least squares fitting procedure (Fig. 8) and the resulting activation parameters are reported in Table 7. The barrier of the helix inversion process for the noranhydro compounds **6** and **7** is lower with respect to the parent compounds **1**–**4**, as expected, and the $\Delta S^{\#}$ values contribute significantly to this decrease. The ring closure reduces the conformational mobility and thus the entropy changes become positive. The more crowded situation occurring in **7**, due to the two methoxy groups, also explains the

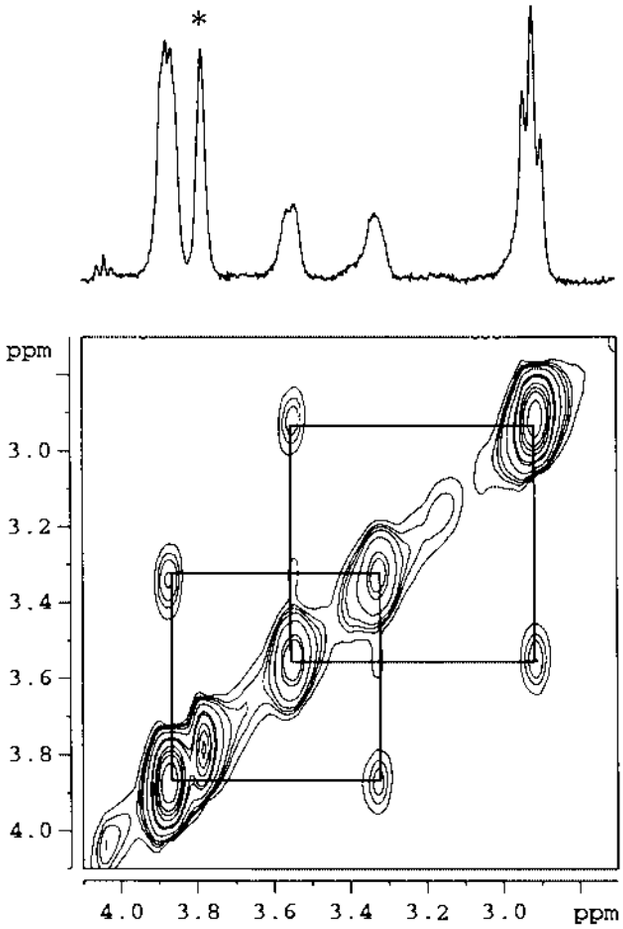

Fig. 6 One of the NOESY-exchange experiments (mixing time t_{mix} 8 ms) performed on **6** (13-H_2 resonances) at the temperature of −93 °C. The starred peak is an impurity of the solvent.

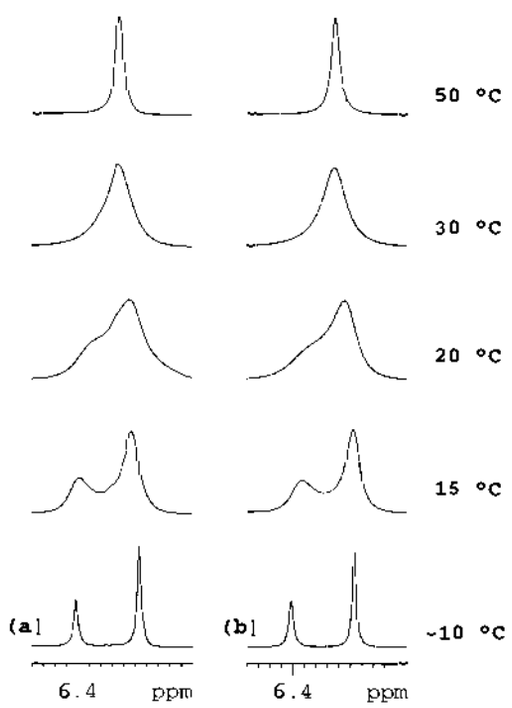

Fig. 7 Selected parts of the (a) experimental and (b) iterated NMR spectra of 5-H proton of noranhydrophleichrome **7** at different temperatures.

higher value of $\Delta G^{\#}$ found for **7** *vs.* **6**, and reproduces the trend observed for the couples **3**, **4** *vs.* **1**, **2**. Therefore, it follows that the helix inversion process is tightly connected with the conformational change of the side-chains, which is a 180° rotation around bond C(1)–C(13) and a 120° rotation around bond C(13)–C(14) for compounds **1**–**5**. In the "6,7-bay" region, the conformational change cannot be proven by experimental data, but MM calculations indicate that the helix inversion is associated with the rotation around the two O–C bonds, as shown by the inversion of the sign of the twist angle C(6)–C(6a)–C(6b)–C(7). In the case of compounds **6**, **7** the inversion of the helix requires the inversion of the five-membered rings, which in fact assume different envelope conformations in the two atropisomers, as shown above.

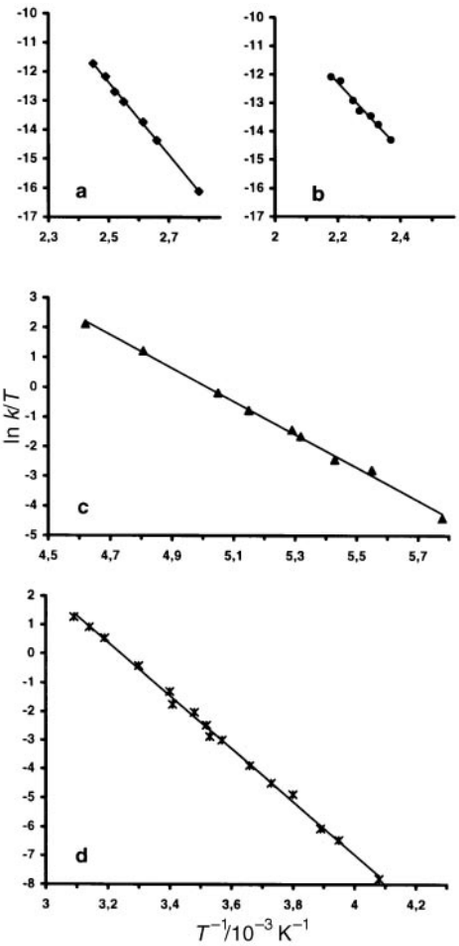

Fig. 8 Least squares fits of ln(k/T) *vs.* temperature ($1/T$) relative to the helix inversion process for (a) cercosporin **1** (r^2 0.9988), (b) phleichrome **3** (r^2 0.9811), (c) noranhydrocercosporin **6** (r^2 0.9971), (d) noranhydrophleichrome **7** (r^2 0.9975).

On the contrary, the helix inversion process is not connected with changes in the tautomeric state, as already observed for cercosporins, phleichromes and hypocrellins[10c,d,h] and in contrast with what was recently published by Petrich and coworkers.[9b] We have studied the tautomeric process in perylenequinones by using the deuterium isotope effect[10e] and the coupling between the proton of the hydrogen bonded OH groups and the adjacent carbon atoms, *i.e.* J(C3,OH) and J(C4,OH).[10d] The coupling constants also allow us to obtain the relative population of each tautomer. We thus applied both methods to noranhydrocercosporin **6** and noranhydrophleichrome **7**. The latter is a good molecule for this investigation, as it shows sharp signals of the two atropisomers at −5 °C. The data obtained (Scheme 1 and Table 5) are similar for both atropisomers. The secondary deuterium isotope effects on ^{13}C chemical shifts (Scheme 2) are spread over the whole perylenequinone system, where the negative sign is characteristic of the quinonoid and the positive one of the benzenoid ring.[10e] This allowed exclusion of a significant presence at the equilibrium

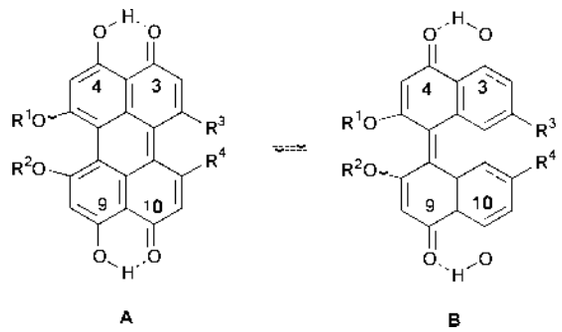

Scheme 1 Tautomeric forms of perylenequinones **1**–**7**.

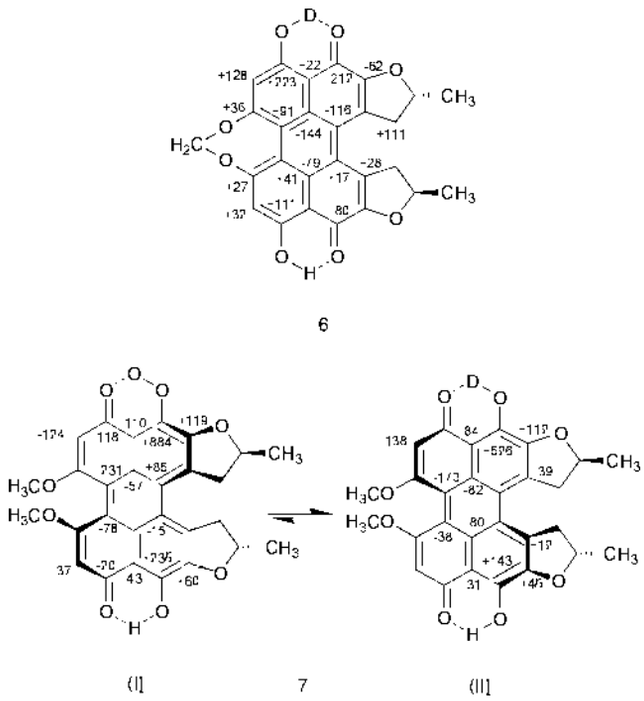

Scheme 2 Secondary deuterium isotope effects on ^{13}C chemical shifts of **6** and **7**.

of cross-quinone tautomers, like 3,10-dihydroxyperylene-4,9-dione, as also found for **1**–**4**.[10d] The strong positive $^{2}\Delta$ effects for C-3 indicate that tautomer **B** is prevailing. This is confirmed by the coupling constant values (Table 5), which show that the relative population of tautomers[10d] is 30% (**A**) and 70% (**B**) for both atropisomers of **7**. In contrast, for noranhydrocercosporin **6** tautomer **A** is prevailing (>95%), as in the parent compound **1**. Although the data for **6** were obtained at 25 °C, *i.e.* in a regime of fast exchange, we can conclude that this occurs for both atropisomers of **6**, because both the coupling constants and the isotope effects are very similar to those obtained for **1**.[10d,e]

Conclusions

The combined use of coupling constants and NOE data allowed us to obtain the conformational preference of the side-chains in the "1,12-bay" region for perylenequinones **1**–**5**. Specifically, the rotation around bond C(1)–C(13) is constrained by steric hindrance, so that the dihedral angles C(2)–C(1)–C(13)–H(13a) and C(12b)–C(1)–C(13)–H(13b) assume values of about 30°, as follows from the two-bond and three-bond $J_{C,H}$. The rotation around bond C(13)–C(14) is less restricted and thus the side-chains have a certain mobility, resulting in all the three main conformations becoming populated. However, some of these conformers are selectively preferred; cercosporin **1** and phleichrome **3** prefer the *gauche*$^{+}$ and the *gauche*$^{-}$ conformation respectively (referred to as the Me–C_1 relationship), even though the *trans* conformation is also present. In contrast, isocercosporin **2** and isophleichrome **4** prefer the *trans* conformation. Cercosporin monoacetate **5** shows for the non-acetylated chain the same situation as cercosporin **1**, while for the acetylated chain the three conformers appear equally populated.

Quantitative NOE experiments on the asymmetric cercosporin monoacetate **5** allowed us to obtain the distance values between protons of the two different chains. From these data we derived a family of structures for **5** in solution, which all present a helical shape with the twist angles C(1)–C(12b)–C(12a)–C(12) and C(6)–C(6a)–C(6b)–C(7) of −36° and −15° respectively. MM/MD calculations showed that this family of conformations, called "propeller", are more stable than the one called "double butterfly" (*i.e.* with twist angles of −30° and +20°) by 7.2 kJ mol^{-1}.

The thermal inversion of the helix in cercosporin **1** and phleichrome **3** is a slow process even at elevated temperatures and the atropisomers **2** and **4**, respectively, can be isolated, but the barrier of the process cannot be estimated by dynamic NMR experiments. The activation parameters thus obtained by traditional kinetic experiments show significant negative values of the entropy change. This can be attributed to the change of conformation of the side-chains in the interconversion process and can explain the long half-time of isomerisation. The higher barrier found for the couple **3**–**4** *vs.* **1**–**2** reflects the more crowded situation occurring in the "6,7-bay" region. Cyclisation of the side-chains in the noranhydro derivatives **6** and **7** reduces the barrier and the inversion process was thus studied by NOE-exchange and dynamic NMR. In particular, the favourable entropy change, which becomes positive for both **6** and **7**, significantly contributes to the decrease of the barrier.

The structure and the conformational preference of both the atropisomers of **6** and **7** were deduced by NMR at low temperature, CD spectra and molecular modelling. The conformational mobility of the five-membered rings is here reduced to an "out of plane" oscillation of only one atom, C-14. Of the two envelope conformations, called α and β, one is more stable (at −80 °C) and thus preferred in the case of noranhydrocercosporin **6**, specifically form α for the more abundant *M(R),14R,17R* atropisomer. For the less abundant one, *P(S),14R,17R*, the two forms are present in fast equilibrium, but with relative populations of *ca.* 70% (α) and 30% (β). In the case of noranhydropheichrome **7**, the more abundant *M(R),14S,17S* atropisomer prefers form β, whereas the less abundant one, *P(S),14S,17S*, prefers form α.

The inversion of the helix is tightly connected with the conformational change of the side-chains, or with the inversion of the five-membered rings, as well as with the conformational change in the "6,7-bay" region, and all the motions must be concerted. In contrast, the helix inversion process is not connected with a change in the tautomeric state. The experimental data (isotope effects and coupling constant values) show the following relative population of tautomers for both the atropisomers of **7**: 30% (**A**) and 70% (**B**). For noranhydrocercosporin **6**, tautomer **A** is prevailing (>95%), as in the parent compound **1**. All the tautomers are in fast equilibrium with respect to the NMR timescale.

Experimental

All reagents and solvents were reagent grade or were purified by standard methods before use. Column chromatography was carried out on flash silica gel Merck 230–400 mesh. TLC analysis and PLC were conducted on silica gel plates (Merck $60F_{254}$). Mass spectra were recorded at an ionising voltage of 70 eV on a Finnigan TQ70 spectrometer.

Monoacetylcercosporin (5). To cercosporin **1** (20 mg) dissolved in CH_2Cl_2, DMAP (5 mg) and pyridine (0.3 cm^3) were

added; the mixture was stirred at 0 °C and a solution of Ac_2O (0.5 cm^3) in CH_2Cl_2 was added dropwise until **1** appeared on TLC to be converted (*ca.* 50%) into a new polar compound; the solution was washed with water, dried, evaporated, and chromatographed on a PLC plate with CH_2Cl_2–MeOH (15 : 1) as eluent. The upper band was 14-(or 17)-monoacetylcercosporin **5** (8 mg) as a red powder; HREIMS: *m*/*z* 576.1560 (calc. for $C_{31}H_{28}O_{11}$ 576.1620), MALDI-MS: *m*/*z* 578 (M + 2). NMR δ_H (acetone-d_6) 7.07 and 7.08 (s, 5- and 8-H), 4.18 and 4.23 (s, 2 × OMe), 1.54 (s, 17-OAc), 5.93 (s, OCH_2O), 0.48 and 0.63 (d, J 6.1, 15- and 18-H_3), 2.89 and 3.68 (dd, 13-H_2), 3.45 (qd, ^2J 6.1, 14-H), 3.13 and 3.71 (dd, 16-H_2), 4.65 (qd, ^2J 6.1, 17-H).

NMR δ_C (acetone-d_6) 136.63 and 134.80 (ddd, C-1 and C-12), 153.82 and 153.63 (qdd, $J_{C,OMe}$ not measured, C-2 and C-11), 182.85 and 182.75 (s, C-3 and C-10), 167.06 and 167.08 (dd, $J_{C4,H5}$ 3.6, $J_{C4,OH}$ 5.0, C-4 and C-9), 109.03 and 109.09 (dd, ^1J 165.8, $J_{C5,OH}$ 7.0, C-5 and C-8), 108.05 and 108.25 (dd, $J_{C3a,OH}$ = $J_{C3a,H5}$ = 5.2, C-3a and C-9a), 164.38 and 164.24 (td, ^3J 6.7, ^2J 3.2, C-6 and C-7), 113.39 and 113.44 (d, ^3J 4.9, C-6a and C-6b), 131.93 and 132.02 (dd, C-12a and C-12b), 128.79 and 128.90 (s, C-12c and C-9b), 93.84 (t, ^1J 170.5, OCH_2O), 61.21 and 61.34 (q, ^1J 146.1, 2-OMe and 11-OMe), 42.92 and 38.39 (m, C-13 and C-16), 67.82 and 70.38 (m, C-14 and C-17), 22.71 and 19.27 (qddd, ^1J 127.6, 15-H_3 and 18-H_3), 169.82 (s, COMe). For *J*s not reported here, see Table 1.

Noranhydrocercosporin (6). Cercosporin **1** (100 mg) was treated at 0 °C with sulfuric acid (0.3 cm^3); after 5 min the mixture was poured into ice–water and the solution extracted twice with EtOAc. Evaporation of the solvent gave a residue that was chromatographed on silica gel (with added 4% KH_2PO_4) with hexane–CH_2Cl_2 (2 : 1). Compound **6** (60 mg) was obtained, EIMS: *m*/*z* 470 $(M + 2)^+$; CD ($c = 4.25 \times 10^{-4}$ mol dm^{-3} in $CHCl_3$): 345, 430, 516 and 557 nm ($\Delta\varepsilon$ +1.4, −2.9, +1.6 and +1.6). The same product was obtained starting from isocercosporin **2**, or from an equilibrium mixture of compounds **1** and **2**. NMR δ_H (20 °C, $CDCl_3$) 7.04 (s, 5- and 8-H), 5.71 (s, OCH_2O), 5.21 (qdd, ^3J 6.0, 9.5 and 8.5, 14-H and 17-H), 3.10 and 3.68 (dd, ^2J 16.0, ^3J 9.5 and 8.5, 13-H_2 and 16-H_2), 1.63 (d, ^3J 6.0, 15-H_3 and 18-H_3), 14.98 (s, 2 chelated OH). NMR δ_C (20 °C, $CDCl_3$), 125.05 (ddd, ^3J 2.0, ^2J 6.8 and 6.8, C-1 and C-12), 15.64 (ddd, ^3J 4.2. 4.2 and 1.6, C-2 and C-11), 177.28 (s, C-3 and C-10), 168.64 (dd, $J_{C4,H5}$ 3.4, $J_{C4,OH}$ 5.0, C-4 and C-9), 109.37 (dd, ^1J 166.4, $J_{C5,OH}$ 6.8, C-5 and C-8), 109.29 (dd, $J_{C3a,H5}$ 3.4, $J_{C3a,OH}$ 5.0, C-3a and C-9a), 164.21 (td, ^3J 6.6, ^2J 4.4, C-6 and C-7), 127.11 (m, C-12a and C-12b), 128.19 (s, C-12c and C-9b), 92.90 (t, ^1J 170.3, OCH_2O), 42.34, (m, C13 and C-16), 81.25 (m, C14 and C-17), 20.85 (qdd, ^1J 127.5, 15-H_3 and 18-H_3). Only a few coupling constant values are reported here, because they are averaged values corresponding to the mixture of the two atropisomers in fast equilibrium; a few $J_{H,H}$ were measured at −80 °C and are reported in Table 4.

Noranhydrophleichrome (7). Phleichrome **3** (25 mg) was reacted as above to obtain **7** (10 mg); mp 300 °C dec.; MALDI-MS: *m*/*z* 487 $(MH)^+$; CD ($c = 4.11 \times 10^{-4}$ mol dm^{-3} in $CHCl_3$): 343, 390, 498 and 534 nm ($\Delta\varepsilon$ +8.2, −6.3, 3.3 and 3.9). The same product was obtained starting from isophleichrome **4**. NMR (20 °C, $CDCl_3$): two atropisomers are visible in these conditions, but the coupling constants were measured at 5 °C; the first figure for each signal refers to the more abundant atropisomer (68%), δ_H 6.38 and 6.40 (s, 5-H, 8-H), 4.00 and 4.05 (s, 6,7-OMe), 4.85 and 5.31 (dq, 14-H,17-H), 3.28 and 3.54 (dd, 13-H_2, 16-H_2), 4.10 and 2.87 (dd, 13-H_2, 16-H_2), 1.79 and 1.27 (d, ^3J 6.0, 15-H_3, 18-H_3), 15.70 and 15.80 (s, chelated OH). NMR: δ_C, 128.55 and 126.41 (ddd, ^2J 6.0 and 6.0, $^3J < 2.0$, C-1, C-12), 151.03 and 150.19 (ddd, ^3J 4.2, 4.2, $^3J < 2.0$, C-2, C-11), 157.18 and 159.77 (d, C-3, C-10), 186.20 and 184.57 (dd, C-4, C-9), 102.36 and 102.01 (dd, ^1J 163, $J_{C5,OH} < 2.0$, C-5, C-8), 108.10 and 107.86 (dd, $J_{C,OH}$ 6.0, $J_{C,H5}$ 4.2, C-3a, C-9a), 120.66 and 119.75 (d, ^3J 6.2, C-6a, C-6b), 168.12 and 167.99 (td, ^3J 4.2, ^2J 3.0, C-6, C-7), 121.89 and 122.68 (m, C-12a, C-12b), 123.54 and 124.20 (s, C-12c, C-9b), 56.35 and 56.41 (q, ^1J 146, 6,7-OMe), 42.65 and 41.08 (m, C-13, C-16), 83.08 and 80.74 (m, 14, C-17), 20.58 and 21.70 (q, broad, ^1J 127, 15-H_3, 18-H_3). For *J*s not reported here see Table 4.

NMR Experiments

The ^1H NMR spectra were recorded on a Bruker AMX 600 spectrometer. The chemical shifts were measured in δ (ppm) and referenced to internal Me_4Si; estimated accuracy ±0.01 ppm. Coupling constants were measured in Hz and are accurate within ±0.1 Hz. The solvents used were [$^2H_6$]acetone, $CDCl_3$, DMSO-d_6 and $CDCl_3$–$CFCl_3$ (30 : 70) for the low temperature experiments. The concentrations were 5–7 mol dm^{-3} for the spectra at high (50 °C) and room temperatures. For those at low temperatures, see Table 5. For the steady-state and transient NOE experiments, standard Bruker pulse sequences were used. The solutions were degassed in the NMR tube by bubbling gaseous N_2 with a capillary glass tube for 5–10 min. For the steady-state experiments the irradiation time was 2 s and the recycling delay 4 s. For the transient experiments a series of mixing times from 100 ms to 1.2 s was used. 2D NOESY spectra were acquired in the phase sensitive TPPI mode, with 2K × 256–512 complex FIDs, spectral width of 12100 Hz, recycling delay of 2 s, 48 scans, at temperatures from −100 to +20 °C. Mixing times from 40 to 600 ms for NOESY, from 20 μs to 600 ms for NOESY-exchange experiments. All spectra were transformed and weighted with a 90° shifted sine-bell squared function to 2K × 512 real data points. The C–H coupling constants were all measured from 1D undecoupled spectra, except for one case noted in Table 1. All *J*s are first order. The assignment of *J*s to specific interactions was made by selective ^1H decoupling. The secondary deuterium isotope effects on ^{13}C chemical shift, measured in ppb, were obtained following the procedure described in ref. 10*e*; solvent $CDCl_3$, temperature 25 °C for **6** and −5 °C for **7**. The temperature for the NMR experiments was measured with the help of NMR-shift thermometers: methanol for low temperatures and ethylene glycol for high temperatures.

Determination of the preferred conformation around bond C(13)–C(14) for compounds 1–5

The molar fractions, x_k, of the rotamers were calculated by solving the appropriate system of equations, with the least-squares method:

$$[A]^T [A] [X] = [A]^T [J^{exp}] \quad (1)$$

where $[A]^T$ is the transposed matrix of $[A]$, $[X]$ is the vector formed by the (unknown) molar fractions, $[J^{exp}]$ is the vector of the experimental J values and $[A]$ is the coefficient matrix formed by the model coupling constants relative to the three rotamers. See eqn. (2), where the two coefficient matrices relate to cercosporins **1**, **2**, **5** and phleichromes **3**, **4** respectively. The goodness of the solution was evaluated by comparing the experimental J values with the calculated ones, obtained from eqn. (1) by introducing the derived molar fractions:

$$[J^{calc}] = [A] [X] \quad (3)$$

1D-transient NOE and 2D-NOESY experiments were used for this conformational analysis. The cross-relaxation rates, obtained by least-squares fitting of the observed NOE intensities, gave the relative distance values by taking as reference the observed NOEs between the geminal protons at C-13 (1.75 Å) and between 14-H and 15-Me (2.5 Å). The conformers corresponding to the calculated three energy minima were used as model geometries for the theoretical NOE calculations, thus

$$|A| = \begin{vmatrix} J^1(11|3R,1114] & J^2(1113R,1114] & J^3(1113R,1114] \\ J^1(11|3S,1114] & J^2(1113S,1114] & J^3(1113S,11|4] \\ J^1(C1,H14] & J^2(C1,H14] & J^3(C1,H14] \\ J^1(C15,H|3R] & J^2(C15,H13R] & J^3(C15,H13R] \\ J^1(C|5,1113S] & J^2(C15,11|3S] & J^3(C15,11|3S] \end{vmatrix} = \begin{vmatrix} 11.4 & 3.2 & 2.0 \\ 2.0 & 11.4 & 3.2 \\ 1.1 & 1.1 & 8.0 \\ 2.1 & 7.9 & 1.1 \\ 1.1 & 2.1 & 7.9 \end{vmatrix} \text{ or } \begin{vmatrix} 2.0 & 3.2 & 11.4 \\ 11.4 & 2.0 & 3.2 \\ 2.1 & 8.0 & 1.1 \\ 1.1 & 7.9 & 2.1 \\ 2.1 & 1.1 & 7.9 \end{vmatrix} \quad (2)$$

creating the $[\sigma]$ matrix for the model σ values. The cross-relaxation rates involving methyls $\sigma_{i,Me}$ were calculated by taking, for each conformation, the arithmetic mean over the three r_{ij}^{-6} values, arising from the three single methyl protons, and finally by averaging over the three conformations, taking into account the experimental values for the relative populations x_k:

$$\langle\sigma_{i,Me}\rangle = A \Sigma_{k=1,3} x_k (\Sigma_{j=1,3} r_{ij}^{-6})/3 \quad (4)$$

where $A = 0.5\ (\mu_0/4\pi)^2\hbar^{-2}\gamma^4\tau_{eff}$ and r_{ij} is the interproton distance. All σ_{ij} values were finally averaged over the three conformations:

$$[\sigma^{calc}] = [X][\sigma] \quad (5)$$

where $[X]$ is the population vector containing the experimental values for the relative populations x_k derived from eqn. (1). The calculated values were then transformed back into "apparent distance" for a direct comparison with the experimental data.

$$[r^{app}_{ij}] = r^{ref}\,[\sigma^{ref}/\sigma_{ij}^{calc}]^{1/6} \quad (6)$$

Determination of the rate constants

For compounds **1**–**4**, kinetic experiments were performed by heating **1** (5 mg) in DMSO (200 mm^3) using a thermostat (±1 °C) at seven different temperatures from 83 to 135.3 °C and collecting samples for NMR measurements, which gave the relative concentrations of the two atropisomers **1** and **2**. The thermometer was calibrated with a platinum thermocouple. The same experiments were performed with **3** in the temperature range 148.7–183.9 °C, thus measuring the relative concentrations of **3** and **4**. The rate constants (k) were calculated by the first-order rate equation:

$$k = 1/t \ln\{(c_0 - c_{eq})/(c_t - c_{eq})\} \quad (7)$$

where $k = k_1 + k_{-1}$ and c_0, c_t and c_{eq} are the concentrations at t_0, t and at the equilibrium.

The rate constants (k) for compounds **6** and **7** were obtained from the NOESY exchange experiments by using the following equations:

$$I_{AA} = 1/2\,[1 + \exp(-2kt_{mix})]\exp(-t_{mix}/T_1^A)\,M_{A0}$$
$$I_{AB} = 1/2\,[1 - \exp(-2kt_{mix})]\exp(-t_{mix}/T_1^B)\,M_{B0} \quad (8)$$

where I_{AA} and I_{AB} are the intensities of diagonal and cross peaks respectively, t_{mix} is the mixing time, M_{A0}, M_{B0} are the equilibrium magnetizations and k is the rate constant corresponding to the reaction of the conversion of the most abundant into the less abundant atropisomer. T_1^A and T_1^B are the longitudinal relaxation times of protons at sites A and B respectively. The temperatures of the experiments (±0.1 °C) were −100, −93, −85 and −79 °C for **6** and −20, −10, 0, +10 and +20 °C for **7**. The rate constants for **6** and **7** were also calculated from the DNMR spectra by the XNMR programs, written by U. Seimet, Germany (available at ftp://acp.chem.uni-kl.de) and Mex written by A. Bain, McMaster University (ftp://zaphod.chemistry.mcmaster.ca). The temperatures of the DNMR experiments were selected in order to complete the set of data and to compare the results of the two methods. The reference half-widths were determined when possible from the signals of non-exchanging molecule protons, or otherwise from the rest proton signals of the solvent. For instance, in the case of compound **6** the width of the solvent peak at −100 °C (7 Hz) was taken as reference ($k = 0$). The spectra were simulated in the slow exchange regime and then iterated by the program to the experimental spectra for each temperature. The resulting k values are in agreement with those obtained by NOESY: compare the values in Table 6 for the temperatures −93, −85 and −79 °C.

Activation parameters

The activation parameters listed in Table 8 were obtained by least-squares fits of $\ln(k/T)$ *vs.* $1/T$ data from the Eyring and the Gibbs–Helmholtz equations.[25,27]

$$\ln k/T = 23.76 - (\Delta H^{\#}/RT) + (\Delta S^{\#}/R) \quad (9)$$

$$\Delta G^{\#} = \Delta H^{\#} - T\Delta S^{\#} \quad (10)$$

Molecular modelling

The inter-proton distances were obtained by use of the Felix software included in the Insight II & Discover programs. Molecular models were built using a Silicon Graphics 4D35GT workstation running the Insight II & Discover software. Molecular mechanics (MM) and molecular dynamics (MD) were carried out using CVFF as forcefield. The starting geometry of cercosporin monoacetate **5** was generated using standard bond lengths and angles and the dihedral angles C(1)–C(12b)–C(12a)–C(12) and C(6)–C(6a)–C(6b)–C(7), named "twist angles" with values of −20 and −10° respectively; the same results were also obtained starting from a planar geometry, *i.e.* with twist angles *ca.* zero. For the starting geometry of the side-chains, we used the preferred conformations obtained from the coupling constant values, *i.e.* the *gauche*$^+$ Me-15/C-1 relationship and the dihedral angles C(2)–C(1)–C(13)–H(13a) = C(12b)–C(1)–C(13)–H(13b) = 30°. The model was then energy minimised using steepest and conjugated gradients until a maximum energy derivative of 4.18×10^{-4} kJ mol^{-1} Å^{-1} was reached. The minimisation was performed without and with the NOE restraints relative to the interactions between protons of the two different chains. The twist angles increased to −36 and −15° respectively ("propeller conformation"). The subsequent restraint molecular dynamics calculations, performed for 10 ps at 1000 K temperature and sampling the trajectory every 1 ps, followed by minimisation with NOE restraints, led to similar results, with twist angles of −38 and −23°. The "double butterfly" conformation cannot be generated starting from a planar geometry, but only by forcing at 16° the twist angle C(6)–C(6a)–C(6b)–C(7). After minimisation, the twist angle C(1)–C(12b)–C(12a)–C(12) reaches the value of −33°. This "double butterfly" conformation, when minimised without the restraints of the C(6)–C(6a)–C(6b)–C(7)

twist angle, leads to the "propeller" conformation (twist angles −36 and 15°), which is more stable than the "double butterfly" by 7.2 kJ mol^{-1}.

Acknowledgements

We are indebted to the University of Milan (FIRST funds) and to the CNR, Agenzia 2000 (G0020A7) for financial support.

References

1 H. Kang and S. E. Rokita, *Nucleic Acids Res.*, 1996, **24**, 3896.
2 G. H. N. Tower, J. E. Page and J. B. Hadson, *Curr. Org. Chem.*, 1997, **1**, 395.
3 R. H. Thomson, *Naturally Occurring Quinones IV Recent Advances*, Blackie Academic & Professional, London, 1997.
4 U. Weiss, L. Merlini and G. Nasini, *Prog. Chem. Org. Nat. Prod.*, l987, **52**, 10.
5 D. C. Dobrowolski and C. S. Foote, *Angew. Chem., Int. Ed. Engl.*, 1983, **22**, 720.
6 A. Arnone, G. Assante, L. Merlini and G. Nasini, *Gazz. Chim. Ital.*, 1989, **119**, 557.
7 E. Kobayashi, H. Nakano, M. Morimoto and T. Tamaoki, *Biochem. Biophys. Res. Commun.*, 1989, **159**, 548.
8 H. Nakano, E. Kobayashi, I. Takahashi, K. Ando, Y. Yoshida, S. Akinaga and T. Iida, Eur. Pat. Appl. EP 284358/88; *Chem. Abstr.*, 1989, **111**, 213336; J. B. Hadson and G. H. N. Towers, *Photochem. Photobiol.*, 1988, **48**, 289.
9 (*a*) H. Falk, *Angew. Chem., Int. Ed.*, 1999, **38**, 3116; (*b*) A. Smirnov, D. B. Fulton, A. Andreotti and W. Petrich, *J. Am. Chem. Soc.*, 1999, **121**, 7979; (*c*) J. W. Lown, *Can. J. Chem.*, 1997, **75**, 99; (*d*) Z. Diwu, *Photochem. Photobiol.*, 1995, **61**, 529; (*e*) F. Gerson, G. Gescheidt, P. Haring, Y. Masur, D. Freeman, H. Spreitzer and J. Daub, *J. Am. Chem. Soc.*, 1995, **117**, 11861.
10 (*a*) L. Merlini, G. Nasini, G. D. Andreetti, G. Bocelli and P. Sgarabotto, *Tetrahedron*, 1982, **38**, 2787; (*b*) A. Arnone, L. Camarda, L. Merlini and G. Nasini, *J. Chem. Soc., Perkin Trans. 1*, 1985, 1387; (*c*) A. Arnone, L. Merlini, R. Mondelli, G. Nasini, E. Ragg and L. Scaglioni, *Gazz. Chim. Ital.*, 1993, **123**, 131; (*d*) A. Arnone, L. Merlini, R. Mondelli, G. Nasini, E. Ragg, L. Scaglioni and U. Weiss, *J. Chem. Soc., Perkin Trans. 2*, 1993, 1447; (*e*) S. Mazzini, L. Merlini, R. Mondelli, G. Nasini, E. Ragg and L. Scaglioni, *J. Chem. Soc., Perkin Trans. 2*, 1997, 2013; (*f*) A. Arnone, U. Brambilla, L. Merlini, G. Nasini and L. Scaglioni, *Gazz. Chim. Ital.*, 1995, **125**, 427; (*g*) A. Arnone, A. Dal Pio Luogo, L. Merlini and G. Nasini, *Liebigs Ann. Chem.*, 1992, 565; (*h*) S. Mazzini, L. Merlini, R. Mondelli and L. Scaglioni, *J. Chem. Soc., Perkin Trans. 2*, 2001, 409.
11 S. Yamazaki and T. Ogawa, *Agr. Biol. Chem.*, 1972, **36**, 1707.
12 D. Mentzafos, A. Terzis and S. E. Philippakis, *Cryst. Struct. Commun.*, 1982, **11**, 71.
13 L. Ernst, V. Wray, V. A. Chertkov and N. M. Sergeyev, *J. Magn. Reson.*, 1977, **25**, 123.
14 R. Wasylishen and T. Schaefer, *Can. J. Chem.*, 1973, **51**, 966.
15 C. A. G. Haasnoot, F. A. A. M. De Leeuw and C. Altona, *Tetrahedron*, 1980, **36**, 2783; A. A. van Beuzekom, F. A. A. M. de Leeuw and C. Altona, *Magn. Reson. Chem.*, 1990, **28**, 68.
16 M. Barfield, *J. Am. Chem. Soc.*, 1980, **102**, 1; M. Barfield, J. L. Marshall and E. D. Canada, Jr., *J. Am. Chem. Soc.*, 1980, **102**, 7.
17 R. Aydin, J. P. Loux and H. Günther, *Angew. Chem., Int. Ed. Engl.*, 1982, **21**, 449; R. Aydin and H. Günther, *Magn. Reson. Chem.*, 1990, **28**, 448.
18 T. Spoormaker and M. J. A. de Bie, *Recl. Trav. Chim. Pays-Bas*, 1980, **99**, 154.
19 Ch. Etzlstorfer, H. Falk and N. Müller, *Monatsh. Chem.*, 1993, **124**, 431.
20 S. Kuyama and T. Tamura, *J. Am. Chem. Soc.*, 1959, **79**, 5726.
21 S. D. Dreher, K. Paruch and T. J. Katz, *J. Org. Chem.*, 2000, **65**, 806.
22 E. Eliel and S. H. Wilen, *Stereochemistry of Organic Compounds*, John Wiley & Sons, New York, 1994.
23 C. A. G. Haasnoot, F. A. A. M. de Leeuw, H. P. M. de Leeuw and C. Altona, *Magn. Reson. Chem.*, 1981, **15**, 43.
24 K. Mukai, K. Daifuku, K. Okabe, T. Tanigaki and K. Inoue, *J. Org. Chem.*, 1991, **56**, 4188; M. Bruce and Y. Roshan-Ali, *J. Chem. Soc., Perkin Trans. 1*, 1981, 2677.
25 F. W. M. Cagle, Jr. and H. Eyring, *J. Am. Chem. Soc.*, 1951, **73**, 562.
26 R. R. Ernst, G. Bodenhausen and A. Wokaun, *Principles of Nuclear Magnetic Resonance in One and Two Dimensions*, Clarendon Press, Oxford, 1987.
27 H. Günther, *NMR Spectroscopy*, John Wiley & Sons, New York, 1995, p. 335.